Chinese Chemical Letters 34 (2023) 107578

Contents lists available at ScienceDirect

Chinese Chemical Letters

journal homepage: www.elsevier.com/locate/cclet

Fluorine-containing drugs approved by the FDA in 2021

Jingrui He[a], Ziyi Li[a], Gagan Dhawan[b,*], Wei Zhang[c,*], Alexander E. Sorochinsky[d], Greg Butler[e], Vadim A. Soloshonok[f,g,**], Jianlin Han[a,*]

[a] Jiangsu Co-Innovation Center of Efficient Processing and Utilization of Forest Resources, International Innovation Center for Forest Chemicals and Materials, College of Chemical Engineering, Nanjing Forestry University, Nanjing 210037, China
[b] Department of Biomedical Science, Acharya Narendra Dev College, University of Delhi, New Delhi 110019, India
[c] Department of Chemistry, University of Massachusetts Boston, Boston, MA 02125, United States
[d] V.P. Kukhar Institute of Bioorganic Chemistry and Petrochemistry, The National Academy of Sciences of Ukraine, Kyiv 02094, Ukraine
[e] Oakwood Chemical, Inc., Estill, SC 29918, United States
[f] Department of Organic Chemistry I, Faculty of Chemistry, University of the Basque Country UPV/EHU, 20018 San Sebastián, Spain
[g] IKERBASQUE, Basque Foundation for Science, Plaza Bizkaia, 48013 Bilbao, Spain

ARTICLE INFO

Article history:
Received 30 March 2022
Revised 29 May 2022
Accepted 1 June 2022
Available online 3 June 2022

Keywords:
Fluorine-containing compounds
Blockbuster drugs
Pharmaceuticals
Anti-cancer
Drug design and development
Asymmetric synthesis

ABSTRACT

Nine new fluorine-containing drugs have been approved by the US Food and Drug Administration (FDA) in 2021, which are presented in this review article. These small molecular drugs feature aromatic fluorine, trifluoromethyl and chlorodifluoro groups. The therapeutic areas of these fluorine-containing drugs include multiple myeloma, lymphoma, HIV, chronic heart failure, chronic myeloid leukemia, (ANCA)-associated vasculitis, migraines, von Hippel-Lindau disease, and non-small cell lung cancer. The brief biological activities and the synthetic methods have been discussed in this review for each of these nine drugs.

1. Introduction

For over 20 years, organo-fluorine molecules represent one of the most fast-growing classes of organic compounds [1–17]. The role of fluorine in the design of pharmaceutical drugs [18–31], agrochemicals, and specialty materials [32–36] is well-recognized. Historically, efforts have been made to incorporate Fluorine into biologically active compounds to develop new pharmaceutical drugs and formulations [18–31]. Scientists pay special attention to the records pertinent to new pharmaceutical drugs and the aspects of their design and therapeutic activity. The goal of this review article is to profile nine new fluorine-containing drugs **1–9** introduced to the market in 2021, which include melphalan flufenamide (Pepaxto™), umbralisib (Ukoniq™), cabotegravir and rilpivirine (Cabenuva™), vericiguat (Verquvo™), asciminib (Scemblix™), atogepant (Qulipta™), avacopan (Tavneos™), belzutifan (Welireg™) and sotorasib (Lumakras™) (Fig. 1). Where it is possible, the mode of biological activity is discussed, emphasizing the specific role of fluorine in the development of a particular drug. For each compound, synthetic routes will be discussed as well as the manner of fluorine introduction into the molecule.

2. Melphalan flufenamide (Melflufen, pepaxto™)

Melflufen **1** is an ester of an alkylated dipeptide, which was developed by Oncopeptides for the treatment of myeloma and amyloid light chain amyloidosis [37]. Melflufen belongs to a new class of peptidase enhancing compounds, which targets the process of multiple myeloma tumor transformation with a unique mechanism. With the use of a simple peptide bond, melflufen's activity is realized by aminopeptidase, resulting in peptidase enhancement effect [38]. Melflufen showed antitumor activity in multiple myeloma, lymphoma and acute myeloid leukemia cell lines, and primary tumor cells [37,39]. Melphalan flufenamide contains a key part of melphalan **10** and a *para*-fluoro-L-phenylalanine (Fig. 2). Structure-activity relationship (SAR) studies disclosed that melphalan flufenamide showed more than ten-fold pharmacological activity compared to melphalan in the cell lines of RPMI 8226, CCRF-CEM and NCI-H69. Although the analogs **11–13** featuring

* Corresponding authors.
** Corresponding author at: Department of Organic Chemistry I, Faculty of Chemistry, University of the Basque Country UPV/EHU, 20018 San Sebastián, Spain
E-mail addresses: gagandhawan@andc.du.ac.in (G. Dhawan), wei2.zhang@umb.edu (W. Zhang), vadym.soloshonok@ehu.es (V.A. Soloshonok), hanjl@njfu.edu.cn (J. Han).

https://doi.org/10.1016/j.cclet.2022.06.001
1001-8417/

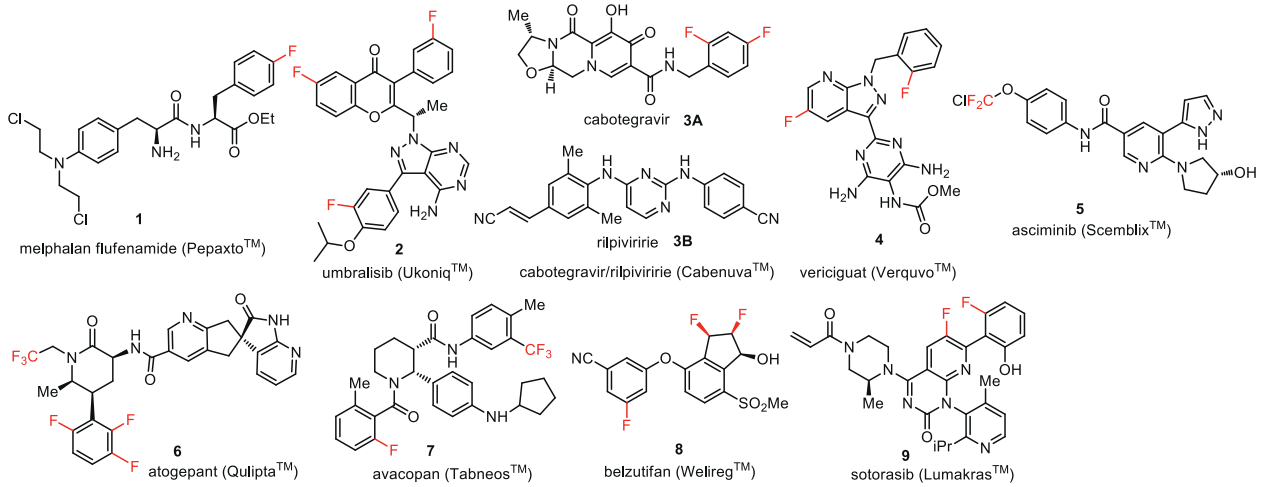

Fig. 1. Structures of approved fluorine-containing drugs.

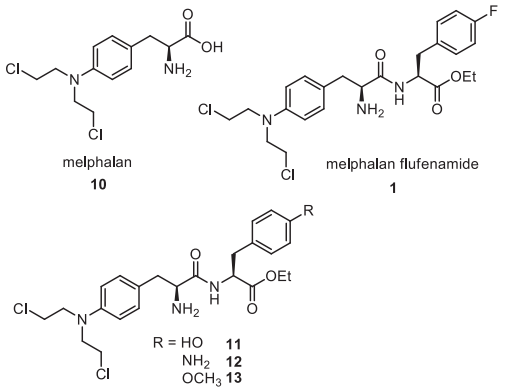

Fig. 2. Structures of melflufen analogs.

other phenylalanine substitutions (hydroxyl, amino and methoxyl) showed very similar activity with that of melphalan flufenamide **1**, the introduction of fluorine substitution increases the metabolic stability [40]. The results of the phase 2 HORIZON study support the US Food and Drug Administration (FDA) to accelerate the approval of melflufen in 2021 for the treatment of three types of refractory multiple myeloma patients [41].

The original chemistry for the synthesis of melphalan flufenamide **1** used melphalan and 4-fluoro-L-phenylalanine ethyl ester as the starting materials. The synthetic strategy was in milligram scale and gave a poor yield of the hydrochloride salt melflufen. However, this method provided enough material for SAR studies [42]. In 2019, Magle Chemoswed developed a safe process for manufacturing of melflufen **1** on a kilogram scale, which was shown in Scheme 1. The condensation reaction between L-Boc-4-nitrophenylalanine (**14**) and L-4-fluoro-phenylalanine ethyl ester hydrochloride salt (**15**) employed 1-(3-dimethylaminopropyl)-3-ethylcarbodiimide hydrochloride (EDC–HCl) and 1-hydroxybenzotriazole (HOBt) as condensation reagents in the presence of *N*-methylmorpholine afforded the amide **16** in 89% yield after 21 h. The amide **16** was reduced using the catalyst Pd/C under hydrogen atmosphere at 35 °C to give the free amine **17** in 83% yield. Reductive alkylation of amine **17** with the use of chloroacetic acid and sodium chloroacetate as the alkylating reagents and borane-dimethyl sulfide as the reductant afforded the intermediate **18**. Treatment with potassium carbonate in ethanol rendered the alkylated intermediate **18** which then underwent deprotection in the presence of HCl in ethyl acetate to generate the target melflufen chloric acid salt **1** at room temperature after 24 h. Notably, alkylated pharmacophores do not involve toxic substances in the whole synthesis process, which makes this method more efficient and safer [43].

3. Umbralisib (Ukoniq™)

Umbralisib **2** a tri-fluorinated chiral compound, was developed by Rhizen and TG Therapeutics as a next-generation of dual phosphoinoside-3-kinase δ inhibitor (PI3Kδ) and casein kinase 1 epsilon inhibitor (CK1ε) [44]. In particular, there are still no known clinically relevant drug-drug interactions observed for umbralisib [45]. Umbralisib has a unique chemical structure (Fig. 3), which contains a 4*H*-chromen-4-one, a 1*H*-pyrazolo[5,4-*d*]pyrimidine and fluorinated phenyl rings. Preclinical analysis showed that umbralisib can effectively inhibit PI3Kδ at a clinically achievable concentration compared with other approved phosphoinoside-3-kinase inhibitors [46]. Umbralisib exhibits great selectivity for the PI3Kδ isoform with more than 1500-fold over α- and β-isoforms ($>$10,000 nmol/L and $>$10,000 nmol/L, respectively, the dissociation constant [K_d] = 6.2 nmol/L) [45]. Umbralisib is unique in the inhibiting of casein kinase 1 epsilon, which plays a key role in the protein translation of oncogenes and may affect the immune regulation of T cells [46].

Rhizen also conducted SAR studies [47–49]. The results disclose that the fluorine substitution on phenyl ring and the absolute configuration play key roles for the inhibitory activity of PI3Kδ and selectivity over PI3K isoforms. For example, IC_{50} (PI3Kδ) value for analog **19** with non-fluoro substitution on 4*H*-chromen-4-one was 13.83 nmol/L, with $>$1000 fold selectivity over PI3Kα. While IC_{50} (PI3Kδ) value for umbralisib **7** is 22.23 nmol/L with more than 10,000 fold over PI3Kα. The (*R*)-isomer **20** showed a decreased activity with an IC_{50} value of 1447 nmol/L [49]. Umbralisib received its first approval from FDA in February 2021 with the trade name as Ukoniq, which is specifically used for the treatment of adult patients with relapsed or refractory marginal zone lymphoma (MZL) [44–50].

Rhizen and TG Therapeutics patented a synthetic method for the preparation of umbralisib **2** with 1*H*-pyrazolo[5,4-*d*]pyrimidine **24** and chiral alcohol **28** as the key intermediates (Scheme 2). The reaction of 4–bromo-2-fluorophenol and isopropanol in the presence of diisopropyl azodicarboxylate (DIAD) and triphenylphosphine produced the ether **21** in 99% yield, which was subjected to a coupling reaction with bis(pinacolato)diboron with [1,1′-bis(diphenylphosphino)ferrocene]dichloropalladium (**II**) as a

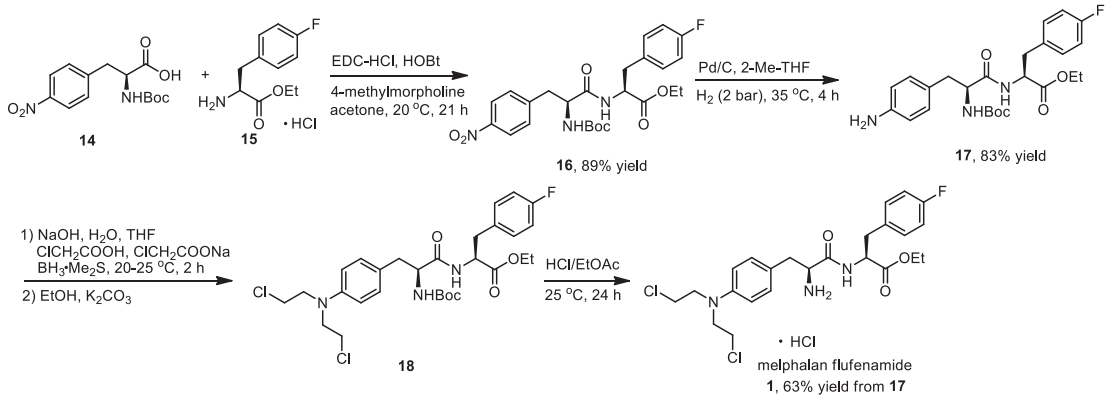

Scheme 1. Synthesis of melphalan flufenamide **1**.

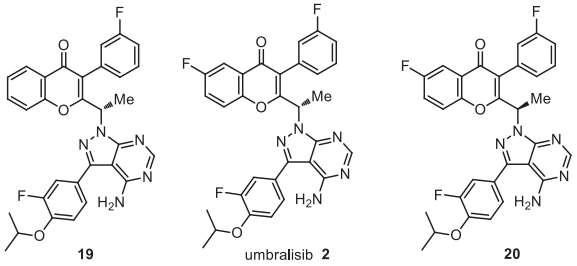

Fig. 3. Structures of umbralisib and analogs.

catalyst resulting in the formation of intermediate **22**. Then, Suzuki coupling reaction between intermediate **22** and 3-iodo-5*H*-pyrazolo[3,4-*d*]pyrimidin-4-amine (**23**) provided the key intermediate **24**.

Friedel-Crafts acylation between 4-fluoroanisole and in situ generated acyl chloride from 3-fluorophenylacetic acid afforded the intermediate **25**, which underwent cyclization reaction with propionic anhydride to give the 4*H*-chromen-4-one intermediate **26** in 52% yield. Treatment of intermediate **26** by *N*-bromosuccinimide (NBS) at 0 °C for 12 h generated intermediate **27**, which then was converted into alcohol **28** in the presence of DMSO and *n*-butanol. Swern oxidation followed by asymmetric reduction by R-alpine borane afforded the (*S*)-alcohol **28** in 94.2% *ee*, which was converted into (*R*)-alcohol **28** *via* two-step conversion. Finally, DIAD-promoted condensation reaction between the two intermediates **24** and (*R*)−**28**, completed the synthesis of umbralisib **2** was obtained in 20% yield [48].

4. Cabotegravir and rilpivirine (Cabenuva™)

Cabenuva (cabotegravir and rilpivirine, injectable formulation) is a long-acting (extended release) regimen, which is a combina-

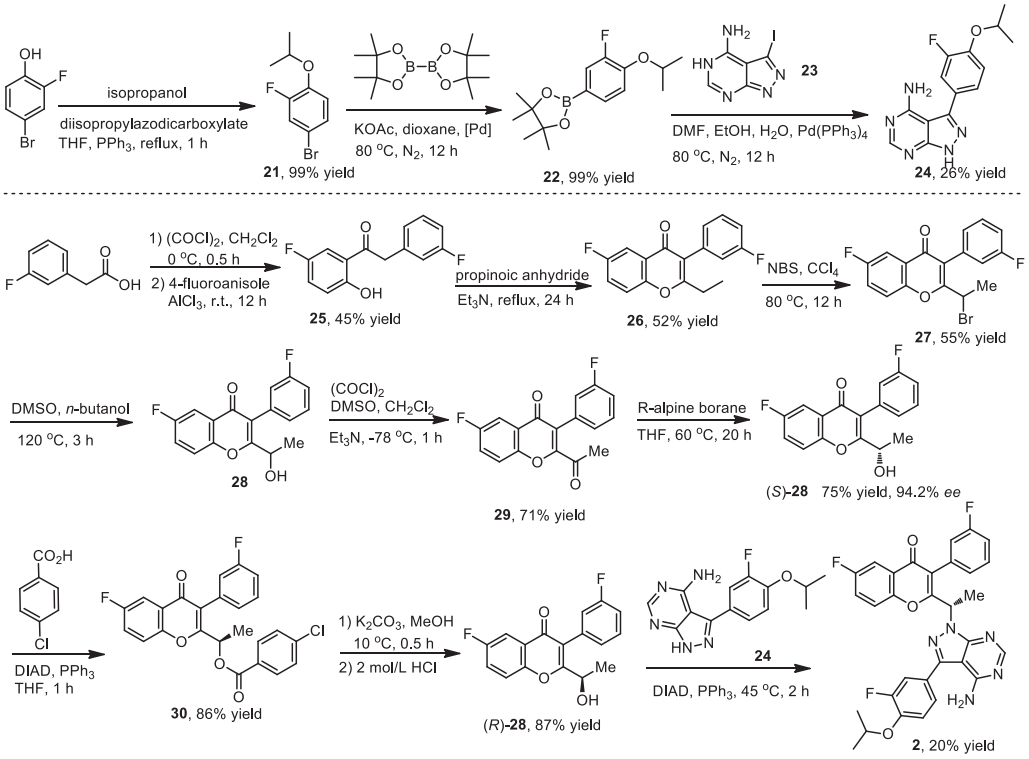

Scheme 2. Synthesis of umbralisib **2**.

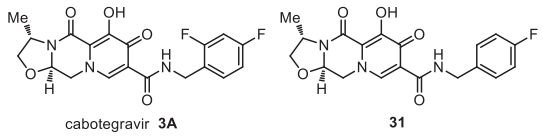

Fig. 4. Structures of cabotegravir and analog.

tion of the integrase strand transfer inhibitor (INSTI) cabotegravir, developed by ViiV Healthcare, and the non-nucleoside reverse transcriptase inhibitor (NNRTI) rilpivirine, developed by Janssen Sciences Ireland UC. It received its first approval in March 2020 in Canada [51,52], and was approved by the FDA in January 2021 for the treatment of HIV infection.

Cabotegravir **3A** is a new long-acting parenteral and a highly effective integrase inhibitor with a half-life of 54 days, allowing parenteral administration every other month. Cabotegravir features low water solubility, high activity, long half-life and slow metabolic clearance [53]. Another advantage of cabotegravir relies on its main metabolization by uridine diphosphate glucuronosyltransferase 1A1, leading to less likely interactions with other antiretroviral drugs [54]. Cabotegravir is a chiral compound which has a flexible six-membered ring, a rigid five-membered ring as its metal chelating scaffold, and a fluorinated benzene ring (Fig. 4) [55]. The SAR studies clearly showed the importance of the incorporation of fluorine substitution into cabotegravir [56]. The introduction of 2-fluoro substituent brought an improved potency by approximately 4-fold compared with its analog **31** ($^{pHIV}IC_{50}$ value = 0.5 nmol/L and 2.1 nmol/L for **3A** and **31** respectively [56].

The synthesis of cabotegravir **3A** was presented in Scheme 3 [57], starting from the readily available chiral alaninol as the key reagent for the introduction of chiral moiety in cabotegravir. As shown in Scheme 3, the pyridone **36** was a key intermediate for this strategy. First, β-keto ester **32** was used as the starting material, which was converted into vinyl amine **33** under reflux in *N*,*N*-dimethylformamide (DMF) and dimethylacetamide (DMA). Next the reaction of amine **33** and aminoacetaldehyde dimethyl acetal provided the vinylogous amine **34**, which underwent cyclization reaction with dimethyl oxalate in the presence of LiOMe which was then hydrolized under basic conditions to yield the key pyridinone intermediate **36**. Intermediate **36** can be successfully transformed into the corresponding aldehyde *via* the treatment of **36** with excess HOAc and catalytic CH_3SO_3H, which reacted with alaninol to construct the oxazolidine ring featuring two chiral carbon centers **37** in 74% yield and 34:1 diastereoselectivity.

Intermediate **37** coupled with 2,4-difluorobenzylamine in the presence of *N*,*N*'-carbonyldiimidazole (CDI) gave the amide **38**. Treatment of **38** with various magnesium salts in acetonitrile led to completely selective C-6 demethylation to afford the desired cabotegravir **3A** in 93% yield. This synthesis is highlighted by the efficient construction of highly functionalized pyridinone nuclei and the highly diastereoselective formation of acyl oxazolidine moieties [57,58].

Another component of cabenuva is rilpivirine **3B**, which is a diaryl pyrimidine non-nucleoside reverse transcriptase inhibitor that inhibits HIV-1 reverse transcriptase through non-competitive binding. In the United States, rilpivirine is recommended in combination with other antiretroviral drugs for the treatment of HIV-1 infected adult patients. Rilpivirine was previously approved by FDA in 2011 with the drug name Edurant [59,60], approved with emtricitabine/tenofovir disoproxil fumarate with the drug name Complera in 2011, and approved in 2017 with dolutegravir with the drug named Juluca for the treatment of HIV-1 infection in adults.

The synthesis of rilpivirine was shown in Scheme 4, using 2-thioxo-2,3-dihydropyrimidin-4(1*H*)-one as the starting material. Intermediate 2-(methylthio)pyrimidine-4(1*H*)-ones **40** was easily prepared by *S*-alkylation of thiouracil **39** with methyl iodide in the presence of sodium hydroxide. Intermediate **40** was condensed with 4-cyanoaniline at 180–190 °C for about 8 h under solvent-free conditions to provide 4-(4-oxo-1,4-dihydropyrimidin-2-ylamino)benzonitriles **41**, which was chlorinated to 4-(4-chloropyrimidin-2-ylamino)benzonitriles **42** *via* refluxing with $POCl_3$ for 30 min [61]. Substitution of intermediate **42** with 4–bromo-2,6-dimethylaniline at 150 °C for 1 h gave the aryl bromide **43**. Finally, the Heck reaction between the aryl bromide **43** and acrylonitrile afforded the corresponding rilpivirine **3B** [62].

5. Vericiguat (Verquvo™)

Vericiguat **4**, also named BAY 1021189, was developed by Bayer and Merck as a soluble guanylate cyclase (sGC) stimulator for treating the disease of chronic heart failure [63,64]. Vericiguat is also an important enzyme in nitric oxide signaling pathway. When nitric oxide binds to guanylate cyclase, vericiguat catalyzes the synthesis of intracellular cyclic guanosine phosphate. Vericiguat is a class II drug of biopharmaceutical classification system with low solubility, low clearance, high permeability, and weak alkalinity [65]. Vericiguat contains a fluorinated 1*H*-pyrazolo[3,4-*b*]pyridine unit, a fluorinated phenyl ring, a pyrimidine-triamine, and a methyl carbamate moiety (Fig. 5). The SAR studies by Bayer showed that the introduction of an additional fluorine atom in vericiguat led to good activity. Good bioactivity was observed with MEC value of 0.3 μmol/L compared with 0.7 μmol/L of the analog **44** with one fluorine substitution (MEC: minimal effective concentration to achieve stimulation of cGMP formation in a recombinant sGC-overexpressing cell line) [66,67]. Vericiguat was first approved by the FDA in 2021 with the trade name as Verquvo for use in patients with symptomatic chronic heart failure (HF) to reduce the risk of cardiovascular death and HF hospitalization [63,68].

Bayer developed a synthetic strategy for the preparation of vericiguat **4** with 2,2,3,3-tetrafluoro-1-propanol as the starting material, which was shown in Scheme 5 [66]. Initially, 2,2,3,3-tetrafluoro-1-propanol **45** was activated by trifluoromethanesulfonic anhydride and followed by the treatment with morpholine at 5 °C to give the fluoroalkylated morpholine **46** in 84% yield. The intermediate **46** was methylated with methyl methanesulfonate at 135 °C to yield the quaternary ammonium intermediate **47**, which underwent an elimination reaction in the presence of sodium hydroxide. The salt **48** was converted to unsaturated aldehyde **49** *via* treatment with morpholine and triethylamine. Acrolein derivative **49** reacted with ethyl 5-amino-1-(2-fluorobenzyl)-1*H*-pyrazole-3-carboxylate **50** in the presence of MsOH and LiCl in refluxing ethanol to form the ester intermediate **51** in 81% yield. Ester **51** was converted into amide **52** *via* the reaction with formamide, and dehydrated with $POCl_3$ to yield the nitrile **53**, which was further converted into amidine **54**. The amidine **54** reacted smoothly with (*E*)-2-(phenyldiazenyl)malononitrile **55** in the presence of trimethylamine to afford the intermediate **56** featuring a pyrimidine ring. Intermediate **56** was subjected to a Pd-catalyzed reduction reaction under a hydrogen atmosphere in DMF, then reacted with methyl chloroformate to give the target vericiguat **4**.

6. Asciminib (Scemblix™)

The BCR-ABL1 oncoprotein is responsible for the progression of chronic myelogenous leukemia (CML). The drug resistance issue is related to the available tyrosine kinase inhibitor therapy targeting ATP-binding site of BCR-ABL1 in patients with Philadelphia chromosome-positive (Ph+) CML. Asciminib **5** was developed by Novartis pharmaceuticals as a potent and selective allosteric ABL1 inhibitor. The US FDA has approved asciminib as an oral drug for the treatment of Philadelphia chromosome-positive

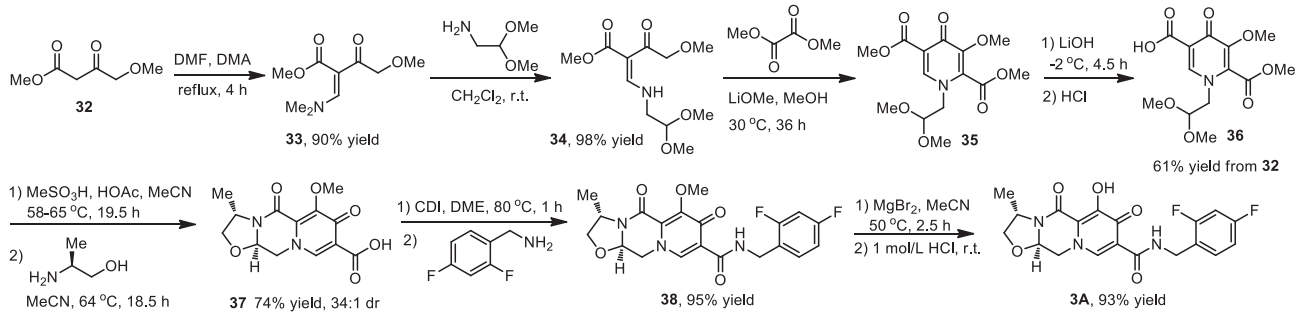

Scheme 3. Synthesis of cabotegravir **3A**.

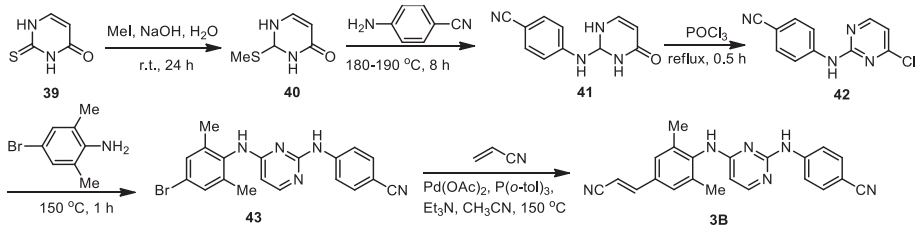

Scheme 4. Synthesis of rilpivirine **3B**.

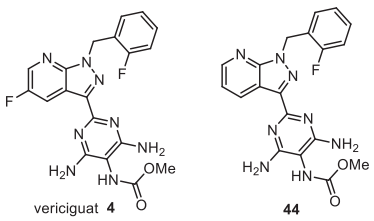

Fig. 5. Structure of vericiguat and analog.

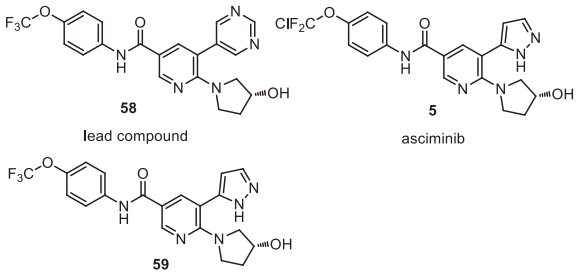

Fig. 6. Structure of asciminib and analogs.

chronic myeloid leukemia for patients with CML and Ph+ acute lymphoblastic leukaemia in October 2021 [69–71]. This compound may also treat or prevent non-malignant diseases associated with abnormally activated ABL1 kinase enzyme [72–74].

Asciminib has a unique CF_2ClO- group in its structure (Fig. 6). The SAR study showed that a *p*-CF_3O- group on the phenyl ring is important for the biological activity (**58**, ABL1 $IC_{50} = 2.3$ nmol/L) [75]. The X-ray co-crystal structure analysis showed that the CF_3O- moiety sits in the myristate pocket in an orthogonal position with respect to the plane of the phenyl ring and the fluorine atom interacts with the carbonyl carbon of leucine-359. Those analogs have increased potency in biochemical and cellular assays. Introducing hydroxyl group in the pyrrolidine ring increased the solubility, but decreased the cellular activity. The pyrimidine ring (**58**, ABL1

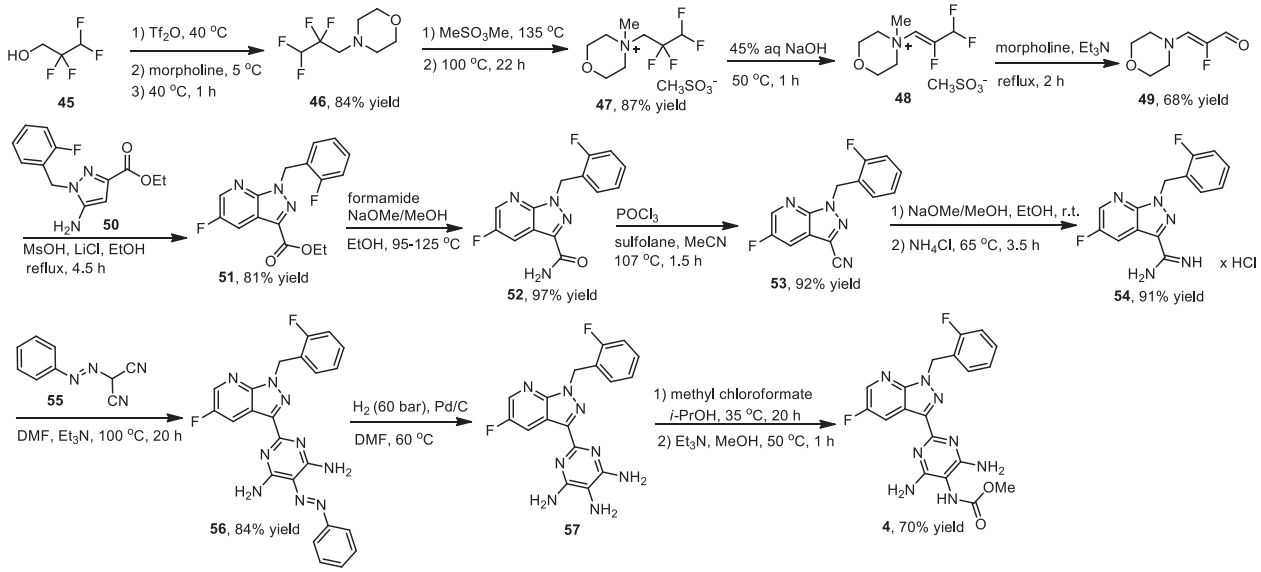

Scheme 5. Synthesis of vericiguat **4**.

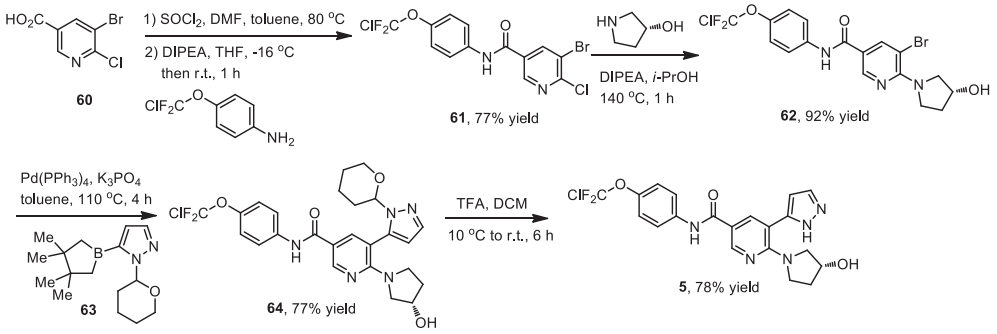

Scheme 6. Synthesis of asciminib **5**.

$IC_{50} = 2.3$ nmol/L) closed to the backbone carbonyl group of glutamic acid-481 was replaced with 5-membered heterocyclic rings such as pyrazole afforded asciminib **5** showing an IC_{50} value of 0.5 nmol/L. Molecular modeling studies showed that the bulkier group can easily be accommodated by either replacing the oxygen atom with a sulfur atom or replacing one of the fluorine atoms with a chlorine (**59**, ABL1 $IC_{50} = 1.1$ nmol/L) [76].

The synthetic route for asciminib **5** was shown in Scheme 6 [76]. 5-Bromo-6-chloronicotinic acid (**60**) was converted into the acid chloride by the reaction with $SOCl_2$ in DMF at 80 °C for 1 h. Then, the concentrated reaction mixture was treated with 4-(chlorodifluoromethoxy)aniline in tetrahydrofuran (THF) in the presence of *N*,*N*-diisopropylethylamine (DIPEA) at room temperature for 1 h to afford compound **61** in 77% yield. Compound **61** reacted with the enantiomerically pure suspension of (*R*)-pyrrolidin-3-ol in *i*-PrOH in the presence of DIPEA at 140 °C for 1 h to afford bromonicotinamide **62** in 92% yield. The Suzuki−Miyaura coupling of **62** with protected boronic ester **63** in the presence of $Pd(PPh_3)_4$ and K_3PO_4 at 110 °C for 4 h afforded the tetrahydropyranyl-protected pyrazole analog **64**, which was then deprotected with TFA at 10–25 °C for 6 h to provide asciminib **5** in 78% yield. It should be mentioned that the starting 4-(chlorodifluoromethoxy)aniline is commercially available.

7. Atogepant (Qulipta™)

Calcitonin gene-related peptide (CGRP) is a potent naturally occurring 37-amino acid neuromodulatory peptide localized in the central and peripheral nervous system, which is responsible for several biological actions, including vasodilation. Studies have shown that CGRP receptors are expressed in regions in the brain associated with migraine pathophysiology and CGRP levels are elevated during migraine attacks. It exerts its biological response by binding to specific cell surface receptors coupled to the activation of the adenylyl cyclase enzyme [77–79]. In clinical trials, the CGRP antagonist is effective in treating acute attacks of migraine and other neurogenic inflammation and inflammatory pain [80,81]. Several labs have reported that the vascular effects of CGRP can be reduced or reversed by a CGRP antagonist [82–87]. Merck conducted a SAR study leading to the identification of atogepant **6**, as a potent and selective CGRP antagonist. It is the first orally administered calcitonin gene-related peptide (CGRP) antagonist, approved by the US FDA in September 2021 for the prevention of episodic migraine and cluster headache. As shown in Fig. 1, two fluorinated groups, trifluorophenyl and trifluoromethyl, are presented in atogepant **6**.

Shown in Scheme 7 was the synthesis of atogepant **6** using fluorinated 2-phenylacetic acid **65** as a starting material [88,89]. Acid **65** in DMF and isopropyl acetate (*i*PAc) was converted to acid chloride by reacting with $POCl_3$ at 0 °C for 30 min. The resulting mixture was added into a solution of K_2CO_3 and NHMe(OMe)·HCl in water below 8 °C to afford **66** in 99% yield. The $CeCl_3$ promoted reaction between intermediate **66** and MeMgCl in THF, followed by treatment with hydrochloric acid (2 mol/L) and methyl *tert*–butyl ether (MTBE) at 5–10 °C to give L-(2,3,6-trifluorophenyl)propan-2-one (**67**) in 95% yield, which was subjected to a substitution reaction with isopropyl *N*-(*tert*–butoxycarbonyl)-*O*-(methylsulfonyl)serinate (**68**) in the presence of $ZnBr_2$ and *t*BuOLi affording the intermediate **69** in 67% yield after 24 h. Asymmetric cyclization reaction of intermediate **69** in the presence of sodium tetraborate decahydrate, *i*PrNH$_2$, pyridoxal-5-phosphate (PLP) and SEQ ID No. 1 in borate buffer at 55 °C for 24 h afforded the carbamate intermediate **70** as a mixture of *cis* and *trans*-isomers (71% yield). The crude mixture of **70** in Me-THF was treated with *t*BuOK at room temperature for 2 h and crystalized in *i*PAc/heptane at 60 °C to afford crystalized *cis*-**70** in 85% yield. The introduction of a trifluoroethyl group with the use of trifluoroethyl trifluoromethanesulfonate and followed by removal of Boc group generated the free amine **71** in 92% yield. Compound **71** coupled with carboxylic acid **72** in the presence of HOBt monohydrate and EDC hydrochloride at room temperature for 4 h giving compound **6** in 95% yield as monohydrate.

8. Avacopan (Tavneos™)

The complement system plays a crucial role in the clearance of immune complexes and the disproportionate activation of the complement system can be manifested in various disorders leading to severe inflammation and tissue damage [90–93]. The anaphylactic complement C5a is the most potent inflammatory mediator acting via its interaction with the membrane-bound C5a receptor (C5aR) [94–99]. Several labs have reported non-peptide-based C5a receptor antagonists [100,101]. The pathogenesis of ANCA-associated vasculitis is characterized by neutrophil based inflammation of small vessels, often including those in the kidney. It is reported that the activation of the alternative complement pathway plays a role in disease pathogenesis [102–104]. The US FDA approved avacopan **7** in October 2021, for the treatment of anti-neutrophil cytoplasmic antibody (ANCA)-associated vasculitis. Avacopan is a small molecule developed by ChemoCentryx, antagonizes complement-dependent inflammation through its binding to the C5aR [105]. It has two phenyl rings containing one fluorine and one trifluoromethyl group (Fig. 7). The SAR studies disclosed that the fluoro and trifluoromethyl substitutions were very important for the improvement of bioactivity. They found that C5aR IC_{50} values for compounds **73A** and **73B** were both between 5 and 50 nmol/L, while less than 5 nmol/L was observed for avacopan **7** [106].

A reported synthetic method for the preparation of avacopan **7** was shown in Scheme 8 [107]. Three-component condensation reaction of ethyl 3-(4-nitrophenyl)-3-oxo-propanoate (**73**), (*R*)-2-amino-2-phenylethan-1-ol and acrolein diethyl acetal at 40 °C, fol-

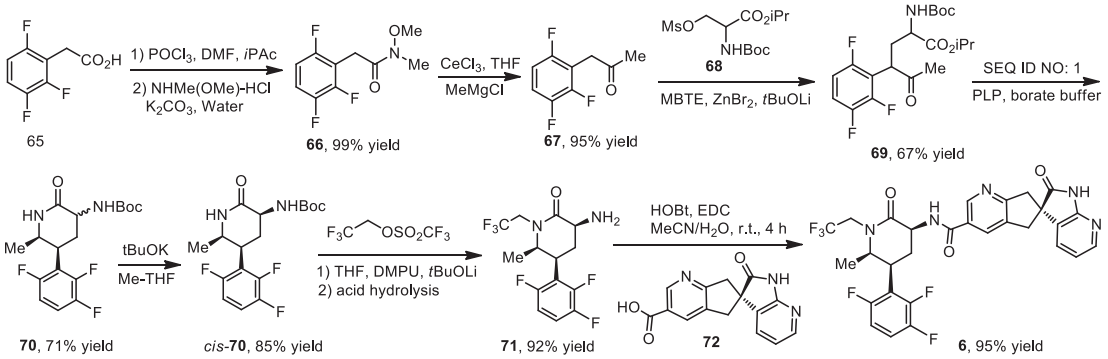

Scheme 7. Synthesis of atogepant **6**.

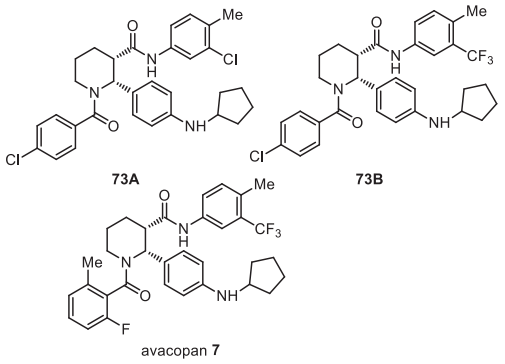

Fig. 7. Structures of avacopan and analogs.

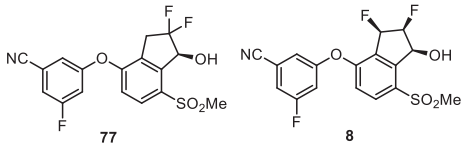

Fig. 8. Structure of belzutifan and analog.

lowed by the treatment of 4 mol/L HCl in dioxane at 70 °C for 22 h generated chiral compound **74** in 38% yield. Reductive amination of compound **74** with cyclopentanone, 10% Pd/C in ethanol in the presence of glacial acetic acid and 12 mol/L HCl, followed by treatment with di-*p*-toluoyl-L-tartaric acid (L-DTTA) provided the intermediate **75**. Amide coupling of **75** with 2-fluoro-6-methylbenzoyl chloride in the presence of K_2CO_3 in water and MTBE as co-solvent afforded the amide **76** in 95% yield. Finally a solution of 4-methyl-5-trifluoromethylaniline and amide **76** in toluene was treated with $AlMe_3$ at 55 °C for 8 h to provide avacopan **7**, which was recrystallized from ethanol/water to give avacopan **7** as white crystals in 80% yield.

9. Belzutifan (Welireg™)

The von Hippel-Lindau (VHL) disease is a rare genetic disorder associated with a high risk of multiple organ cancer development [108,109]. Renal cell carcinoma (RCC) is characterized by the inactivation of the tumor suppressor VHL protein, a component of an E3 ubiquitin ligase complex responsible for protein degradation. A major role of VHL protein is the regulation of the hypoxia-inducible factors (HIF). The hypoxia-inducible factor 2α (HIF-2α) is a critical factor in renal cell carcinoma (RCC). Oxygen-dependent HIF prolyl-hydroxylase enzyme controls the cellular activity of HIF-2α [110,111]. In the presence of oxygen, these enzymes hydroxylate specific proline residues to provide a substrate recognition site for VHL protein and target it for rapid proteasomal degradation. The VHL protein is defective or absent in patients with RCC which leads to the accumulation and transcriptional activation of HIF-2α.

A number of research groups have reported that the inner pocket in HIF-2α could be allosterically inhibited by small molecules and thus the reduced protein–protein interaction between HIF-2α and ARNT leads to the inhibition of transcriptional activity [112–115]. The first generation HIF-2α inhibitor **77** developed through structure-guided studies have shown clinical activity in advanced RCC patients [116] but its use was restricted due to its extensive phase 2 metabolism *via* glucuronide conjugation [117–119]. The structural modification of **77** to belzutifan **8** by altering its geminal difluoro group to a vicinal difluoro group resulted in enhanced potency, decreased lipophilicity, and better ADME profile with reduced formation of the glucuronide conjugate (Fig. 8). The US FDA has approved a hypoxia-inducible factor-2α (HIF-2α) inhibitor, belzutifan (Welireg) developed by Merck), for the treatment of cancers associated with VHL disease that does not require

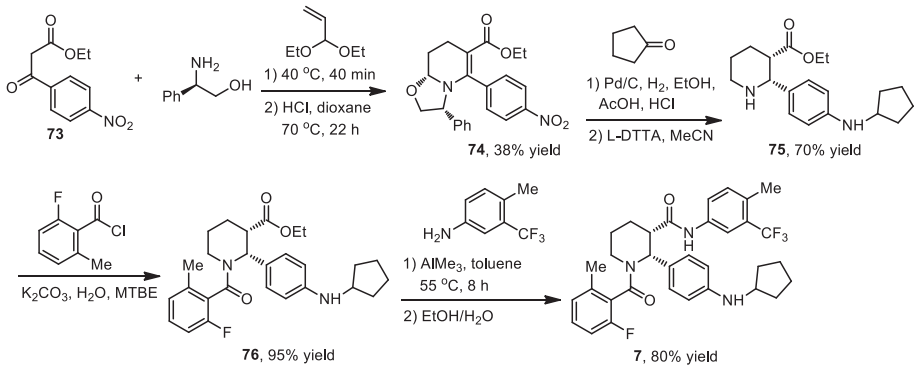

Scheme 8. Synthesis of avacopan **7**.

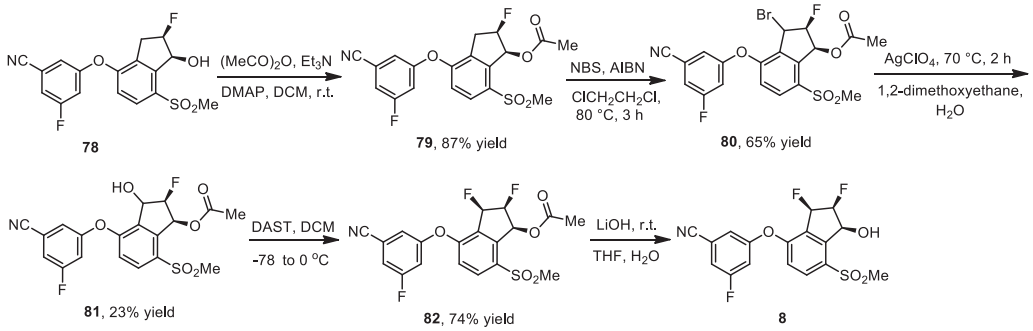

Scheme 9. Synthesis of belzutifan **8**.

immediate surgery. As shown in Fig. 8, belzutifan **8** is a chiral compound featuring three continuous chiral carbon centers, which also contains three fluorine substitutions, two C(sp^3)-F and one C(sp^2)-F.

The synthesis of belzutifan **8** was outlined in Scheme 9, which used optically pure fluorinated compound **78** as a starting material [120–122]. The alcohol **78** was converted to acetate ester **79** in 87% yield by reaction with acetic anhydride in the presence of 4-(dimethylamino)pyridine (DMAP) and trimethylamine. The ester **79** was then brominated by a radical reaction initiated by azodiisobutyronitrile (AIBN) with the use of *N*-bromosuccinimide (NBS) at 80 °C for 3 h resulting in the compound **80** in 65% yield. The treatment of **80** with $AgClO_4$ at 70 °C for 2 h gave the alcohol **81** in 23% yield. Subsequently, stereoselective fluorination reaction of **81** with (diethylamino)sulfur trifluoride (DAST) at −78 °C gave the vicinal difluoro compound **82** (74% yield). Finally, the ester group in compound **82** was hydrolyzed by 0.5 mol/L LiOH solution at 0 °C to afford belzutifan **8**.

10. Sotorasib (Lumakras™)

RAS is a family of three ubiquitously expressed small GTPases in all animal cell types. Many RAS-driven human tumors are associated with the mutations in the RAS gene family. Of the various isoforms like KRAS, HRAS, and NRAS, the KRAS mutation is the most frequently occurring. The KRAS protein is a signaling molecule capable of downstream regulation of the proliferation of tumors, and the mutations mostly occur in the codon 12 like p.G12D (41%), p.G12V (28%), and p.G12C (14%) [123–126]. A series of compounds have been explored as KRAS p.G12C inhibitors interacting with the cryptic pocket of the target protein (H95, Y96, and Q99) [127]. Among them, quinazolinone analogs have demonstrated good biochemical and cellular potency. The isopropylphenyl moiety of quinazolinones bonded perfectly with the crucial residues of the cryptic pocket. Molecular docking suggested that the fluorophenol moiety occupying a hydrophobic pocket region could form hydrogen bonding to Arg68 to enhance the potency and MDCK permeability [128–130]. Sotorasib **9** was developed by Amgen as a selective and irreversible covalent inhibitor b that interacts with the sulfur atom of the cysteine residue present in the KRas mutant known as KRas G12C [131]. Sotorasib **9** contains two C(sp^2)-F moieties on different aromatic rings (Fig. 9). SAR studies by Amgen showed that replacing the C6 chloro substituent of compound **83** with a fluoro substituent overcame the consistently low bioavailabilities although a modest loss of activity in cellular assays was observed (p-ERK $IC_{50} = 68$ nmol/L and 11 nmol/L for sotorasib **9** and **83** respectively) [130]. The US FDA grants accelerated the approval of sotorasib in May 2021 for KRAS G12C mutated NSCLC with the trade name Lumakras™ [131].

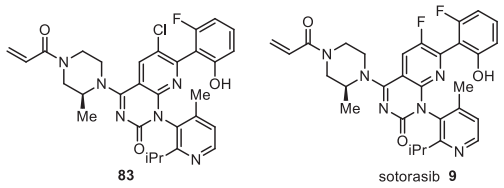

Fig. 9. Structure of sotorasib and analog.

The synthesis of sotorasib **9** using 2,6-dichloro-5-fluoronicotinic acid, as a starting material was shown in Scheme 10 [130,132].

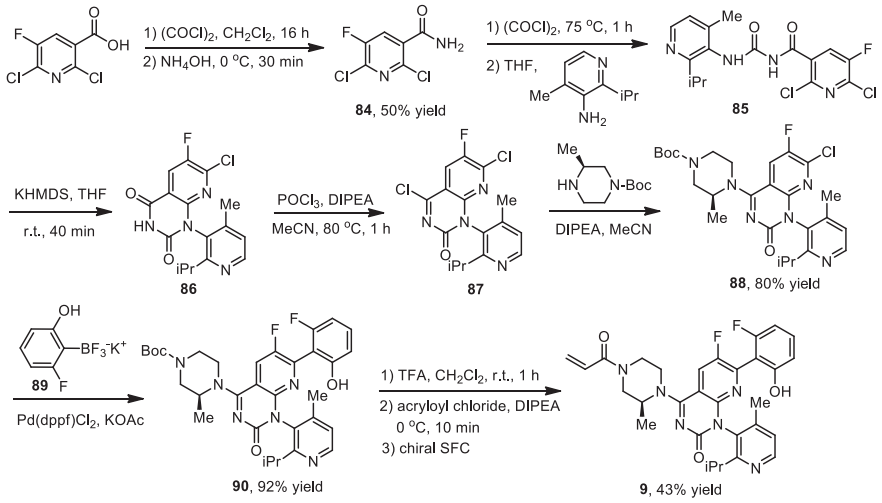

Scheme 10. Synthesis of optically pure sotorasib **9**.

2,6-Dichloro-5-fluoronicotinic acid was converted to acid chloride by reacting with oxalyl chloride in DCM for 16 h, which then reacted with NH_4OH in dioxane at 0 °C for 30 min to give 50% yield of nicotinamide **84**. Treatment of **84** with oxalyl chloride 75 °C for 1 h and followed by reaction with 2-isopropyl-4-methylpyridin-3-amine at 0 °C for 1 h yielded the intermediate **85**, which was subjected to an intramolecular cyclization reaction in the presence of 1,1,1,3,3,3-hexamethyldisilazane potassium salt (KHMDS) at room temperature to afford cyclic intermediate **86**. Compound **86** was chlorinated with $POCl_3$ in the presence of DIPEA at 80 °C to the chlorinated intermediate **87** which was used without further purification. Reaction of **87** by (*S*)-4-Boc-2-methyl piperazine with DIPEA as a base afforded **88** in 80% yield. Pd-catalyzed coupling of **88** with potassium trifluoroborate salt **89** in the presence of KOAc afforded **90** in 92% yield. Compound **90** was deprotected via treatment with TFA, acrylation with acryloyl chloride in the presence of DIPEA, and chiral separation by chiral supercritical fluid chromatography (SFC) purification afforded the targeted **9** in 43% yield.

11. Conclusions and outlook

The fluorine editing of drug-candidate molecules is regarded as one of the most promising strategies in the development of modern pharmaceuticals. Last year the FDA approved fifty new small-molecules drugs among which, nine compounds featured fluorine-containing groups. These include Pepaxto (**1**), Ukoniq (**2**), Cabenuva (**3**), Verquvo (**4**), Scemblix (**5**), Qulipta (**6**), Tavneos (**7**), Welireg (**8**) and Lumakras (**9**), representing such therapeutic areas as multiple myeloma, lymphoma, HIV, chronic heart failure, chronic myeloid leukemia, (ANCA)-associated vasculitis, migraines, von Hippel-Lindau disease, non-small cell lung cancer, respectively. This review has covered the aspect of biological activity and the most significant synthetic approaches for the preparation of these new pharmaceuticals. As compared with previous years [26–28], one can notice a significant increase of compounds with multiple fluorine substitutions, including aliphatic (**5**, **6**, **8**)/aromatic (**1**, **2**, **4**, **7**, **9**) as well as different types of aromatic fluorine on the same molecule (**6**, **7**). This trend indicates a departure from traditional fluorine editing which usually involved a single fluorination. Indeed, the continuous development of fluorine methodology and more deep understanding of the fluorine effect on bio-properties would probably provide strong support for this trend in the future.

Another striking feature of this new crop of drugs is that virtually all, except for (**4**), are chiral compounds featuring up to three stereogenic centers. Considering the necessity of application of chiral drugs in enantiomerically pure form, critical improvements in asymmetric synthesis and characterization of chiral fluorine-containing compounds have to be made. Thus, studying the self-disproportionation of enantiomers (SDE) properties of these chiral drugs is an important issue, which is recommended in the fluorine-containing drug manufacture [133–138].

Declaration of competing interest

The authors declare no conflicts.

Acknowledgments

We gratefully acknowledge the financial support from the National Natural Science Foundation of China (No. 21761132021), the Qing-Lan Project of Jiangsu Province (for Han) and IKERBASQUE, Basque Foundation for Science (for Soloshonok).

References

[1] R.E. Banks, V. Murtagh, H.M. Marsden, R.G. Syvret, J. Fluorine Chem. 122 (2001) 271–275.
[2] X.Y. Yang, T. Wu, R.J. Phipps, F.D. Toste, Chem. Rev. 115 (2015) 826–870.
[3] R.G. Syvret, K.M. Butt, T.P. Nguyen, V.L. Bulleck, R.D. Rieth, J. Org. Chem. 67 (2002) 4487–4493.
[4] M. Reichel, K. Karaghiosoff, Angew. Chem. Int. Ed. 59 (2020) 12268–12281.
[5] P. Bravo, M. Guidetti, F. Viani, et al., Tetrahedron 54 (1998) 12789–12806.
[6] X. Xu, K. Matsuzaki, N. Shibata, Chem. Rev. 115 (2015) 731–764.
[7] H. Ohkura, D.O. Berbasov, V.A. Soloshonok, Tetrahedron 59 (2003) 1647–1656.
[8] K. Gondo, T. Kitamura, Molecules 17 (2012) 6625–6632.
[9] J. Han, A.E. Sorochinsky, T. Ono, V.A. Soloshonok, Curr. Org. Synth. 8 (2011) 281–294.
[10] R.G. Syvret, W.J. Casteel, G.S. Lal, J.S. Goudar, J. Fluorine Chem. 125 (2004) 33–35.
[11] G.V. Röschenthaler, V.P. Kukhar, I.B. Kulik, et al., Tetrahedron Lett. 53 (2012) 539–542.
[12] M.S. Wiehn, E.V. Vinogradova, A. Togni, J. Fluorine Chem. 131 (2010) 951–957.
[13] M. Shevchuk, Q. Wang, R. Pajkert, et al., Adv. Synth. Catal. 363 (2021) 2912–2968.
[14] E. Merino, C. Nevado, Chem. Soc. Rev. 43 (2014) 6598–6608.
[15] J.A. Ma, D. Cahard, J. Fluorine Chem. 128 (2007) 975–996.
[16] S.S. Li, J. Wang, Acta Chim. Sin. 76 (2018) 913–924.
[17] J. Hu, K. Ding, Acta Chim. Sin. 76 (2018) 905–906.
[18] E.P. Gillis, K.J. Eastman, M.D. Hill, D.J. Donnelly, N.A. Meanwell, J. Med. Chem. 58 (2015) 8315–8359.
[19] I. Ojima, J. Fluorine Chem. 198 (2017) 10–23.
[20] J. Wang, M. Sánchez-Roselló, J.L. Aceña, et al., Chem. Rev. 114 (2014) 2432–2506.
[21] Y. Zhou, J. Wang, Z. Gu, et al., Chem. Rev. 116 (2016) 422–518.
[22] Y. Zhu, J. Han, J. Wang, et al., Chem. Rev. 118 (2018) 3887–3964.
[23] J. Han, L. Kiss, H. Mei, et al., Chem. Rev. 121 (2021) 4678–4742.
[24] H. Mei, J. Han, K.D. Klika, et al., Eur. J. Med. Chem. 186 (2020) 111826.
[25] H. Mei, J. Han, S. White, et al., Chem. Eur. J. 26 (2020) 11349–11390.
[26] H. Mei, J. Han, S. Fustero, et al., Chem. Eur. J. 25 (2019) 11797–11819.
[27] H. Mei, A.M. Remete, Y. Zou, et al., Chin. Chem. Lett. 31 (2020) 2401–2413.
[28] Y. Yu, A. Liu, G. Dhawan, et al., Chin. Chem. Lett. 32 (2021) 3342–3354.
[29] J. Han, A.M. Remete, L.S. Dobson, et al., J. Fluorine Chem. 239 (2020) 109639.
[30] S. Purser, P.R. Moore, S. Swallow, V. Gouverneur, Chem. Soc. Rev. 37 (2008) 320–330.
[31] C. Isanbor, D. O'Hagan, J. Fluorine Chem. 127 (2006) 303–319.
[32] Q. Wang, H. Song, Q. Wang, Chin. Chem. Lett. 33 (2022) 626–642.
[33] Y. Ogawa, E. Tokunaga, O. Kobayashi, K. Hirai, N. Shibata, iScience 23 (2020) 101467.
[34] T. Fujiwara, D. O'Hagan, J. Fluorine Chem. 167 (2014) 16–29.
[35] C. Qin, W. Liu, Y. Nie, et al., Chin. J. Org. Chem. 40 (2020) 2232–2253.
[36] P. Chen, W. Bai, Y. Bao, J. Mater. Chem. C 7 (2019) 11731–11746.
[37] S. Dhillon, Drugs 81 (2021) 963–969.
[38] M. Wickström, P. Nygren, R. Larsson, et al., Oncotarget 8 (2017) 66641–66655.
[39] M. Fortunato, T. Giovanni, A.M. Enrica, et al., Drug Des. Dev. Ther. 15 (2021) 2969–2978.
[40] F. Lehmann, J. Wennerberg, Melflufen: A journey from discovery to multi-kilogram production, in: J.A. Pesti, A.F. Abdel-Magid, R. Vaidyanathan (Eds.), Complete Accounts of Integrated Drug Discovery and Development: Recent Examples from the Pharmaceutical Industry, Volume 3, ACS Symposium Series, 1369, American Chemical Society, Washington DC, 2020, pp. 157–177.
[41] F. Schjesvold, M. Dimopoulos, S. Delimpasi, et al., Lancet Haematol. 9 (2022) e98–e110.
[42] J. Gullbo, M. Tullberg, J. Våbenø, et al., Oncol. Res. 14 (2003) 113–132.
[43] H. Cotton, B. Bäckström, I. Fritzson, et al., Org. Process Res. Dev. 23 (2019) 1191–1196.
[44] D. Sohita, J.K. Susan, Drugs 81 (2021) 857–866.
[45] H.A. Burris III, I.W. Flinn, M.R. Patel, et al., Lancet Oncol. 19 (2018) 486–496.
[46] N.H. Fowler, F. Samaniego, W. Jurczak, et al., J. Clin. Oncol. 39 (2021) 1609–1618.
[47] M. Muthuppalaniappan, S. Viswanadha, G. Babu, S.K.V.S. Vakkalanka, PT US20110118257 A1, 2011.
[48] M.S. Weiss, H.P. Miskin, P. Sportelli, S.K.V.S. Vakkalanka, PT US 20150290317 A1, 2015.
[49] S.K.V.S. Vakkalanka, M. Muthuppa-Laniappan, D. Nagarathnam, PT WO2014006572 A1, 2014.
[50] A.D. Zelenetz, L.I. Gordon, J.E. Chang, et al., J. Natl. Compr. Canc. Netw. 19 (2021) 1218–1230.
[51] A. Markham, Drugs 80 (2020) 915 –822.
[52] D.A. Margolis, J. Gonzalez-Garcia, H.J. Stellbrink, et al., Lancet 390 (2017) 1499–1510.
[53] T. Zhou, H. Su, P. Dash, et al., Biomaterials 151 (2018) 53–65.
[54] C. Trezza, S.L. Ford, W. Spreen, R. Pan, S. Piscitelli, Curr. Opin. HIV AIDS 10 (2015) 239–245.
[55] S.A. Hassounah, A. Alikhani, M. Oliveira, et al., Antimicrob. Agents Chemother. 61 (2017) 1–9.
[56] A.J. Brian, K. Takashi, G.W. Jason, et al., J. Med. Chem. 56 (2013) 5901–5916.
[57] H. Wang, M.D. Kowalski, A.S. Lakdawala, F.G. Vogt, L. Wu, Org. Lett. 17 (2015) 564–567.
[58] L.H. David, Org. Process Res. Dev. 23 (2019) 716–729.
[59] M. Sanford, Drugs 72 (2012) 525–541.
[60] M. Sharma, L. Saravolatz, J. Antimicrob. Chemoth. 68 (2013) 250–256.
[61] X.Q. Feng, Y.H. Liang, Z.S. Zeng, et al., ChemMedChem 4 (2009) 219–224.

[62] J. Guillemont, E. Pasquier, P. Palandjian, et al., J. Med. Chem. 48 (2005) 2072–2079.
[63] M. Anthony, D. Sean, Drugs 81 (2021) 721–726.
[64] B. Michael, G. Michael, L. Maximilian, et al., Clin. Pharmacokinet. 59 (2020) 1407–1418.
[65] L. Nguyen, D.E. Baker, Hosp. Pharm. (2021), doi:10.1177/00185787211016338.
[66] M. Follmann, J. Ackerstaff, G. Redlich, et al., J. Med. Chem. 60 (2017) 5146–5161.
[67] C. Hirth-Dietrich, P. Sandner, J.P. Stasch, et al., PT WO2011147810 A1, 2011.
[68] A. Alsumali, D. Lautsch, R. Liu, et al., Adv. Ther. 38 (2021) 2631–2643.
[69] E.D. Deeks, Drugs 82 (2022) 219–226.
[70] M. Breccia, G. Colafigli, E. Scalzulli, M. Martelli, Expert Opin. Investig. Drugs 30 (2021) 803–811.
[71] R. Kurzrock, J.U. Gutterman, M. Talpaz, N. Engl. J. Med. 319 (1988) 990–998.
[72] A.A. Wylie, J. Schoepfer, W. Jahnke, et al., Nature 543 (2017) 733–737.
[73] T.P. Hughes, M.D. Michael, J. Mauro, et al., N. Engl. J. Med. 381 (2019) 2315–2326.
[74] S.K. Dodd, P. Furet, R.M. Grotzfeld, et al., PT WO2013171639A1, 2013.
[75] J. Zhang, F.J. Adrian, W. Jahnke, et al., Nature 463 (2010) 501–506.
[76] J. Schoepfer, W. Jahnke, G. Berellini, et al., J. Med. Chem. 61 (2018) 8120–8135.
[77] P.J. Goadsby, L. Edvinsson, R. Ekman, Ann. Neurol. 28 (1990) 183–187.
[78] J.L. Bellamy, R.K. Cady, P.L. Durham, Headache 46 (2006) 24–33.
[79] L.H. Lassen, P.A. Haderslev, V.B. Jacobsen, H.K. Iversen, B. Sperling, J. Olesen, Cephalalgia 22 (2002) 54–61.
[80] J. Olesen, H.C. Diener, I.W. Husstedt, et al., N. Engl. J. Med. 350 (2004) 1104–1110.
[81] K.A. Petersen, L.H. Lassen, S. Birk, L. Lesko, J. Olesen, Clin. Pharmacol. Ther. 77 (2005) 202–213.
[82] H. Doods, G. Hallermayer, D. Wu, et al., Br. J. Pharmacol. 129 (2000) 420–423.
[83] L. Edvinsson, P.J. Goadsby, Cephalalgia 14 (1994) 320–327.
[84] M. Ashina, L. Bendtsen, R. Jensen, et al., Neurology 55 (2000) 1335–1340.
[85] P. Holzer, Neuroscience 24 (1998) 739–768.
[86] A.M. Salmon, M.I. Damaj, L.M. Marubio, et al., Nat. Neurosci. 4 (2001) 357–358.
[87] A. May, M.A. Gamulescu, U. Bogdahn, C.P. Lohmann, Cephalalgia 22 (2002) 195–196.
[88] F. Chen, C. Molinaro, W.P. Wuelfing, et al., PTWO2013169348, 2013.
[89] I.M. Bell, M.E. Fraley, S.N. Gallicchio, et al., PTWO2012064910A1, 2012.
[90] P.F. Kohler, H.J. Müller-Eberhard, J. Immunol. 99 (1967) 1211–1216.
[91] R. Schindler, J.A. Gelfand, C.A. Dinarello, Blood 76 (1990) 1631–1638.
[92] N. Haeffner-Cavaillon, J.M. Cavaillon, M. Laude, M.D. Kazatchkine, J. Immunol. 139 (1987) 794–799.
[93] J.M. Cavaillon, C. Fitting, N. Haeffner-Cavaillon, Eur. J. Immunol. 20 (1990) 253–257.
[94] D.E. van Epps, D.E. Chenoweth, J. Immunol. 132 (1984) 2862–2867.
[95] D.L. Haviland, R.L. McCoy, W.T. Whitehead, et al., J. Immunol. 154 (1995) 1861–1869.
[96] R.A. Wetsel, Immunol. Lett. 44 (1995) 183–187.
[97] R.R. Buchner, T.E. Hugli, J.A. Ember, E.L. Morgan, J. Immunol. 155 (1995) 308–315.
[98] D.E. Chenoweth, T.E. Hugli, Proc. Natl. Acad. Sci. U. S. A. 75 (1978) 3943–3947.
[99] J. Zwirner, A. Fayyazi, O. Götze, Mol. Immunol. 36 (1999) 877–884.
[100] H. Sumichika, K. Sakata, N. Sato, et al., J. Biol. Chem. 277 (2002) 49403–49407.
[101] A.J. Strachan, T.M. Woodruff, G. Haaima, D.P. Fairlie, S.M. Taylor, J. Immunol. 164 (2000) 6560–6565.
[102] D.R.W. Jayne, P.A. Merkel, T.J. Schall, P. Bekker, N. Engl. J. Med. 384 (2021) 599–609.
[103] D.R.W. Jayne, A.N. Bruchfeld, L. Harper, et al., J. Am. Soc. Nephrol. 28 (2017) 2756–2767.
[104] K.J. Warrington, N. Engl. J. Med. 384 (2021) 664–665.
[105] A. Lee, Drug 82 (2022) 79–85.
[106] P. Fan, K.L. Greenman, M.R. Leleti, et al., PT WO 2011163640 A1, 2011.
[107] P. Fan, J. Kalisiak, A. Krasinski, et al., PT US 9745268 B2, 2017.
[108] E.D. Deeks, Drugs 81 (2021) 1921–1927.
[109] T.K. Choueiri, T.M. Bauer, K.P. Papadopoulos, et al., Nat. Med. 27 (2021) 802–805.
[110] P. Jaakkola, D.R. Mole, Y.M. Tian, et al., Science 292 (2001) 468–472.
[111] R.K. Bruick, S.L. McKnight, Science 294 (2001) 1337–1340.
[112] T.H. Scheuermann, D.R. Tomchick, M. Machius, et al., Proc. Natl. Acad. Sci. U. S. A. 106 (2009) 450–455.
[113] T.H. Scheuermann, Q. Li, H.W. Ma, et al., Nat. Chem. Biol. 9 (2013) 271–276.
[114] J.L. Rogers, L. Bayeh, T.H. Scheuermann, et al., J. Med. Chem. 56 (2013) 1739–1747.
[115] T.H. Scheuermann, D. Stroud, C.E. Sleet, et al., J. Med. Chem. 58 (2015) 5930–5941.
[116] P.W. Wehn, J.P. Rizzi, D.D. Dixon, et al., J. Med. Chem. 61 (2018) 9691–9721.
[117] E.M. Wallace, J.P. Rizzi, G. Han, et al., Cancer Res. 76 (2016) 5491–5500.
[118] H. Cho, X. Du, J.P. Rizzi, et al., Nature 539 (2016) 107–111.
[119] W. Chen, H. Hill, A. Christie, et al., Nature 539 (2016) 112–117.
[120] R. Xu, K. Wang, J.P. Rizzi, et al., J. Med. Chem. 62 (2019) 6876–6893.
[121] T.K. Choueiri, R.J. Motzer, N. Engl. J. Med. 376 (2017) 354–366.
[122] J.A. Josey, R. Shrimali, E.M. Wallace, T. Wong, PT WO2019191227, 2019.
[123] A.D. Cox, S.W. Fesik, A.C. Kimmelman, J. Luo, C.J. Der, Nat. Rev. Drug Discov. 13 (2014) 828–851.
[124] G.A. Hobbs, C.J. Der, K.L. Rossman, J. Cell Sci. 129 (2016) 1287–1292.
[125] I.A. Prior, P.D. Lewis, C. Mattos, Cancer Res. 72 (2012) 2457–2467.
[126] J. Canon, K. Rex, A.Y. Saiki, et al., Nature 575 (2019) 217–223.
[127] J.M. Ostrem, U. Peters, M.L. Sos, J.A. Wells, K.M. Shokat, Nature 503 (2013) 548–551.
[128] T. Pantsar, Sci. Rep. 10 (2020) 11992.
[129] X. Xiao, M. Lai, Z.H. Xie, et al., Eur. J. Med. Chem. 213 (2021) 113082.
[130] B.A. Lanman, J.R. Allen, J.G. Allen, et al., J. Med. Chem. 63 (2020) 52–65.
[131] H.A. Blair, Drugs 81 (2021) 1573–1579.
[132] A.T. Parsons, M. Beaver, PT WO 2021097212, 2021.
[133] A.E. Sorochinsky, T. Katagiri, T. Ono, et al., Chirality 25 (2013) 365–368.
[134] J. Han, D.J. Nelson, A.E. Sorochinsky, V.A. Soloshonok, Curr. Org. Synth. 8 (2011) 310–317.
[135] A.E. Sorochinsky, J.L. Aceña, V.A. Soloshonok, Synthesis (Mass) 45 (2013) 141–152.
[136] J. Han, O. Kitagawa, A. Wzorek, K.D. Klika, V.A. Soloshonok, Chem. Sci. 9 (2018) 1718–1739.
[137] J. Han, A. Wzorek, K.D. Klika, V.A. Soloshonok, Molecules 26 (2021) 2757.
[138] J. Han, R. Dembinski, V.A. Soloshonok, K.D. Klika, Molecules 26 (2021) 3994.